THOMAS PROCESS AND WAVE FUNCTION IMAGING IN P-HE TRANSFER IONIZATION INVESTIGATED BY COLTRIMS

V. Mergel[1,*], R. Dörner[1], M. Achler[1], Kh. Khayyat[1], O. Jagutzki[1], L. Spielberger[1], A. Salin[2], C.J. Wood[3], R.E. Olson[3], Dž. Belkić[4], C.L. Cocke[5], J.H. McGuire[6] and H. Schmidt-Böcking[1]

[1]Institut für Kernphysik, Universität Frankfurt, August-Euler-Str.6, D-60486 Frankfurt, Germany.
[2]CNRS and Université Bordeaux, F-33405 Talence, France.
[3]University of Missouri-Rolla, Missouri 65401, USA.
[4]Atomic Physics, Stockholm University, Frescativ. 24, S-104 05 Stockholm, Sweden.
[5]Kansas State University, Manhattan, 66506 Kansas, USA.
[6]Tulane University, New Orleans, Louisiana, USA.

INTRODUCTION

One of the fundamental capture mechanisms for fast ion atom collisions was proposed by L.H. Thomas in 1927[1] based on a classical treatment and observed by Palinkas *et al.*[2] for the first time. This Thomas process can be understood as two consecutive binary collisions, first by the projectile with one of the target electrons and, second, between this electron and either the target nucleus (*e*-*N*-Thomas-scattering) or another target electron (*e*-*e*-Thomas-scattering). The *e*-*e*-Thomas-scattering offers a unique possibility to investigate dynamic electron-electron- (*e*-*e*-) correlation in atomic collision processes. For fast proton impact the perturbation of the target (in our case helium) is small and the electrons are quickly removed from the bound state by the *e*-*e*-Thomas-scattering. The *e*-*e*-Thomas-scattering always leads to a double ionization of the target, while the capture can either be to a bound (transfer ionization, TI) or a continuum state of the projectile[3]. Thus this process will leave the nucleus behind with its momentum distribution from the initial ground state, which mirrors the sum momentum of the 2 electrons. Furthermore the absolute probability for that process yields information on the spatial distribution of the two electrons.

In this paper we report on a kinematically complete experiment for the transfer ionization reaction (TI) 0.15 – 1.4MeV $p + He \rightarrow H^0 + He^{2+} + e^-$ using Cold Target Recoil Ion Momentum Spectroscopy (COLTRIMS). We have measured all three momentum components of the recoiling He^{2+}-ion, with a solid angle of nearly 4π, in coincidence with the polar and azimuthal deflection angle of the outgoing H^0-atom. These 5 momentum components fully determine the final state of the reaction (apart from the spin). The remaining 4 momentum components of the 3 particles in the continuum (H^0, He^{2+}, e^-) are determined by the energy and momentum conservation laws, assuming capture to the ground state[4]. We can clearly

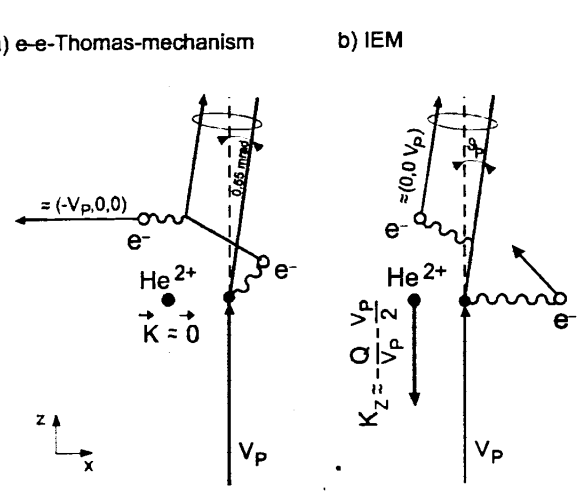

Figure 1. Kinematics of the correlated e-e-Thomas-process (a) and of the two-step process of kinematic capture and ionization by independent projectile electron interactions (b).

separate the 2nd order e-e-Thomas-scattering from the independent two-step process by their different locations in the 9-dimensional momentum space, and thus we can determine the contributions to the total TI cross section for each of them separately. We also provide a very detailed insight in the reaction dynamics by imaging the three-dimensional final state momentum distributions of the recoiling ion and the electron.

EXPERIMENTAL SETUP

We have used **Cold Target Recoil Ion Momentum Spectroscopy** (COLTRIMS)[5, 6, 7, 8] to determine the 3-dimensional momentum vector and the charge states of the recoil ions. The proton beam was collimated to a size of < 0.5mm and a divergence of $< 250\mu$rad. The beam was charge-state selected before and after the target region by different sets of electrostatic deflector plates. A supersonic helium gas jet was used as target. It combines the two most important features necessary for recoil ion spectroscopy: low internal temperature (< 50mK) and localization of the target (diameter 5mm). A residual gas pressure without gas jet of 1×10^{-8}mbar and a target thickness in the jet of 1.5×10^{12}cm^{-2} were obtained. Recoil ions created in the interaction volume with the projectile beam were accelerated by a weak electric field (9V/cm) onto a two-dimensional position sensitive channel-plate detector.

KINEMATICS OF TRANSFER IONIZATION

The mechanisms responsible for non-radiative capture plus ionization can be grouped into two types, depending on whether: (i) mainly the target nucleus or (ii) the continuum electron compensates the momentum change of the projectile, due to the mass transfer by the captured electron.

Process (i) occurs if a target electron is captured by a projectile-target interaction due to a velocity matching between the electron and projectile involving the electronic velocity distributions in the initial and final bound state (kinematic capture), or if an e-N-Thomas-process occurs. From[9] we estimated that the e-N-Thomas-process is negligible for TI at the observed energies. To achieve TI in this process the second electron must also be emitted to the continuum. The second step might involve either a second interaction of the projectile with the target (IEM) (see fig. 1a) or proceed via relaxation of the target wave function (shake-off).

The e-e-Thomas-mechanism (see fig. 1b) is a type (ii) process, which could in principle occur with two initially unbound electrons.

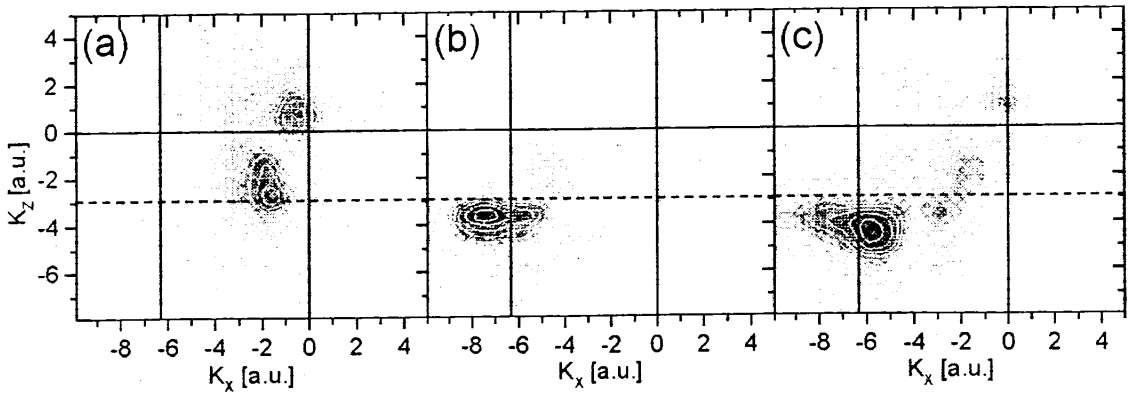

Figure 2. Contour plot of the TDCS $d^3\sigma/(d\theta_P dK_x dK_z)$ as a function of K_x and K_z at a scattering angle of $\theta_P = (0.55 \pm 0.1)$mrad. (a) and (b): present experiment at $E_P = 0.5$MeV (a) and 1MeV (b). (c) and (d): dCTMC-calculation without (c) and with (d) e-e-interaction both at 1MeV. The dashed lines show $K_z = K_0$ (see eq.2) and the left vertical lines show the momentum transfer to the whole target ($-q_x$, see eq.1) corresponding to the scattering angle range of $\theta_P = (0.55 \pm 0.1)$mrad.

For TI momentum conservation reads

$$K_{x,y,z} = -(q_{x,y,z} + k_{x,y,z}), \tag{1}$$

where $K_{x,y,z}$ are the momentum components of the He^{2+}-recoil ion, $k_{x,y,z}$ of the emitted electron and $q_{x,y,z}$ the momentum change of the projectile. x, y denote the two components perpendicular and z the component parallel to the incident projectile. Using energy conservation it follows to first order in Q/E_P and in the ratio between electron and projectile mass for the longitudinal (z) direction[7] (atomic units are used throughout ($e = \hbar = m_e = \alpha c = 1$))

$$K_z = \underbrace{-\frac{Q_t}{v_P} - \frac{v_P}{2}}_{\text{transfer } (K_0)} + \underbrace{\frac{E_e - Q_i}{v_P}}_{\text{ionization}} - k_z \tag{2}$$

with $Q_t + Q_i = Q = \epsilon_{He} - \epsilon_H$, where ϵ_H is the binding energy of the hydrogen atom and $\epsilon_{He}(= -2.9\text{a.u.})$ is that of the helium ground state. E_e is the final continuum energy of the emitted electron. The capture leads predominantly to the ground state of hydrogen ($Q = -2.4$a.u.)[4]. Furthermore rotational symmetry allows us to define $q_x \equiv q_\perp$ for each collision event. Thus x and y denote the components parallel and perpendicular to the projectile scattering plane. Neglecting Q/v_P, the signature for the e-e-Thomas mechanism is

$$\mathbf{q} = (v_P, 0, 0),\ \mathbf{k} = (-v_P, 0, 0) \text{ and } \mathbf{K} = (0, 0, 0) \tag{3}$$

where $q_x = v_P$ corresponds to $\theta_P = 0.55$mrad. while the independent process (i) is expected to appear at $K_z \approx K_0$ [10, 11, 12].

RESULTS AND INTERPRETATION

Recoil Ion Momentum Distributions

Figure 2a shows the experimentally observed triply differential cross section $d^3\sigma/(d\theta_P dK_x dK_z)$ for $\theta_P = (0.55 \pm 0.15)$mrad at $E_P = 1$MeV. Figure 2b represents the dCTMC-calculation for (0.55 ± 0.1)mrad at 1MeV without and (c) with the e-e-interaction (e-e-dCTMC). Figure 2a shows two distinct peaks, one at $K_x = -1.6$a.u. and $K_z = -2.8$a.u. and one at $K_x = -0.4$a.u. and $K_z = 0.7$a.u. The lower peak shows the clear signature of kinematic capture plus independent ionization, while the upper peak corresponds to the e-e-Thomas-mechanism. The slightly positive K_z of the Thomas contribution may be a result from the

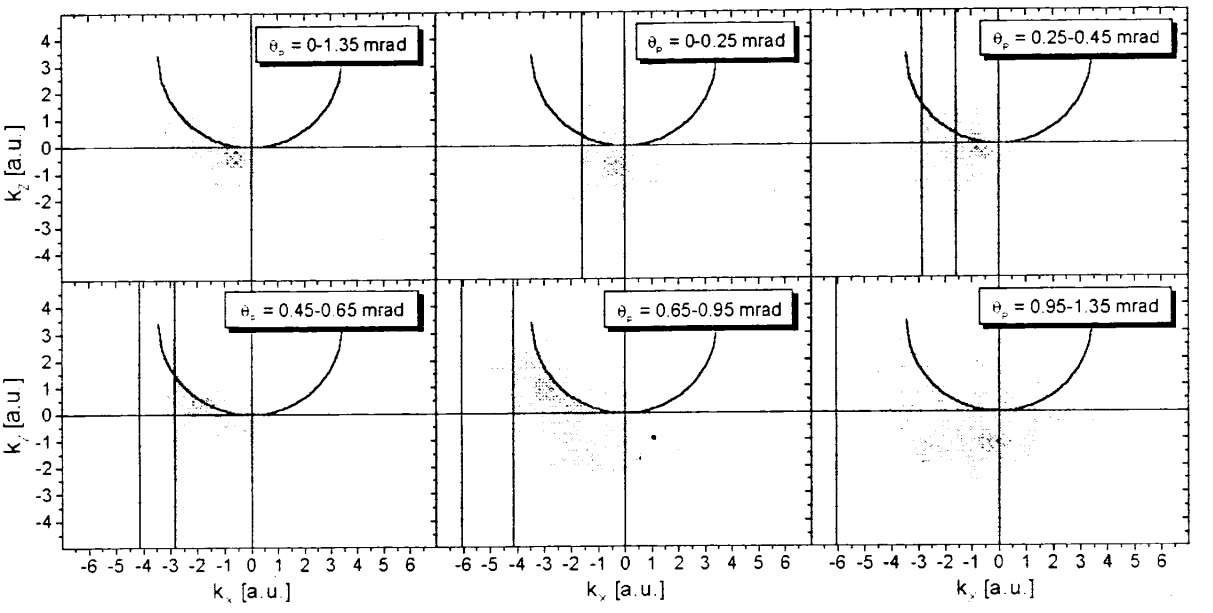

Figure 3. Contour plot of the TDCS $d^3\sigma/(d\theta_P dk_x dk_z)$ at $E_P = 0.3$MeV as a function of k_x and k_z at different scattering angles as indicated in the figure. The left vertical lines show the momentum transfer to the whole target ($-q_x$, see eq.1) corresponding to the scattering angle range of $\theta_P = (0.55 \pm 0.1)$mrad.

neglected Q-value in eqn. 3. The kinematic capture plus independent ionization results in a larger K_x than the e-e-Thomas contribution, because a kinematic capture favors close impact parameters due to the high momentum components required in the initial state. Since the e-e-Thomas-mechanism does not depend on close impact parameters (it is also possible with 2 electrons at rest), it results mainly in small transverse recoil ion momenta.
The 4-body dCTMC calculations include the radial correlation between electrons by a dynamic screening parameter of the target nuclear charge as well as higher orders in the interaction between electrons and the target nucleus (*i.e.* the e-N-Thomas-mechanism). The e-e-dCTMC includes the explicit $1/r_{12}$-potential which is "turned on" exponentially when the total energy of either electron relative to the He nucleus becomes positive, to enable e-e-scattering but avoiding autoionization. The dCTMC calculations show the necessity of an explicit electron-electron interaction potential for the e-e-Thomas-process. However the dCTMC fails to predict details of the momentum space image.

We have extracted the absolute contribution of the e-e-Thomas-scattering from the 4-fold differential cross sections Fitting the function $\sigma = a \times v_P^b$ to the data, we find a $v_P^{-7.4\pm1.0}$-dependence for the e-e-Thomas-process. This is in disagreement with the classical prediction of Thomas[1] and the asymptotic result of the BK2[13, 14], all predicting a v_P^{-11}-dependence. However, we find a good agreement for the e-e-double scattering with a 'post' version of the four-body reformulated impulse approximation (RIA-4B)[15].

Electron Momentum Distributions

Figure 3 shows the momentum distribution of the emitted electron (k_x, k_z) at $E_P = 0.3$MeV in the scattering plane defined by the projectile. The distribution in figure 3a is integrated over $\theta_P = 0 - 1.35$mrad, which covers nearly all of the total cross section. Figure 3b-f shows the electron distribution for different ranges of θ_P as indicated in the figure. We observe a mainly backwards emission with a small transverse momentum k_x both for distant (b) and for very close (f) collisions. Around $\theta_P = 0.55mrad$ (d) an emission along the binary encounter ridge at negative k_x (opposite to the projectile) is found. This electron emission can be understood as an independent two-step mechanism of kinematic capture plus independent binary encounter as proposed by the independent electron model (IEM)[10, 11] shown in fig.1a.

When the momentum transfer to the electron is small (b,f) the reaction dynamics cannot be interpreted in such simple pictures of mechanisms. In these cases the momentum transfer from the projectile to the electron is small, either because the total momentum transfer on the target is small (b) or since the momentum transfer is that large that it can only be caused by a scattering between the two nuclei. ($\theta_P = 0.55$mrad this is the maximum possible momentum transfer from a proton to an electron at rest). For both cases the emission looks similar and is peaked straightly backwards. Investigating different E_P (not shown here), we find that with increasing E_P the backwards momentum of the electron increases. This fact is interpreted as an effect of an angular correlation in the initial state. The kinematic capture probes a part of the initial state wave function where the captured electron has already a large forward momentum component. For this part of the wave function the other electron may have a momentum distribution which is mainly backwards peaked.

In conclusion we have performed a kinematically complete experiment on the proton on helium transfer ionization using **COLTRIMS**. It enables us to distinguish clearly between the e-e-Thomas-scattering and the independent two-step process in the 9-dimensional momentum space of the final state. From this we obtained the absolute contribution of the Thomas-process to the TI cross section. The imaging of the momentum distributions of the recoil ion and the electron opens a deep insight on the collision dynamics. Only some examples of the results could be demonstrated in this paper

ACKNOWLEDGMENTS

This work was supported by DFG, BMBF, DAAD, EG, Freunde und Förderer der Universität Frankfurt, Studienstiftung des Deutschen Volkes, DOE Office of Fusion Energy, Alexander von Humboldt Foundation and the Wenner-Gren Science Foundation. We thank our colleagues and friends R. Dreizler, S. Keller, J.M. Rost, J. Burgdörfer, R. Schuch and L.C. Cocke for many helpful discussions.

* email: mergel@ikf.uni-frankfurt.de

REFERENCES

1. L.H. Thomas. *Proc. Roy. Soc.*, A114:561–76, 1927.
2. J. Palinkas, R. Schuch, H. Cederquist, and O. Gustafsson. *Phys. Rev. Lett.*, 63(22):2464–67, 1989.
3. Jamal Berakdar. PhD thesis, Universität Freiburg, 1992.
4. Robert Gayet and Antoine Salin. *J. Phys.*, B20:L571–76, 1987.
5. R. Dörner, V. Mergel, R. Ali, U. Buck, C.L. Cocke, K. Froschauer, O. Jagutzki, S. Lencinas, W.E. Meyerhof, S. Nüttgens, R.E. Olson, H. Schmidt-Böcking, L. Spielberger, K. Tökesi, J. Ullrich, M. Unverzagt, and W. Wu. *Phys. Rev. Lett.*, 72:3166–69, 1994.
6. V. Mergel, R. Dörner, J. Ullrich, O. Jagutzki, S. Lencinas, S. Nüttgens, L. Spielberger, M. Unverzagt, C.L. Cocke, R.E. Olson, M. Schulz, U. Buck, E. Zanger, W. Theisinger, M. Isser, S. Geis, and H. Schmidt-Böcking. *Phys. Rev. Lett.*, 74:2200–2203, 1995.
7. Volker Mergel. PhD thesis, Universität Frankfurt/Main, ISBN 3-8265-2067-X, Shaker Verlag, Aachen, Germany, 1996.
8. J. Ullrich, R. Moshammer, R. D"orner, O. Jagutzki, V. Mergel, H. Schmidt-Böcking, and L. Spielberger. *J. Phys.*, B30:2917, 1997. *Topical Review.*
9. E. Horsdal-Pedersen, C.L. Cocke, and M. Stöckli. *Phys. Rev. Lett.*, 50:1910–13, 1983.
10. Antoine Salin. *J. Phys.*, B22:3901–14, 1989.
11. Robert Gayet and Antoine Salin. *Nucl. Instr. Meth.*, B56/57:82–85, 1991.
12. V. Mergel, R. Dörner, M. Achler, Kh. Khayyat, S. Lencinas, J. Euler, O. Jagutzki, S. Nüttgens, M. Unverzagt, L. Spielberger, W. Wu, R. Ali, J. Ullrich, H. Cederquist, A. Salin, R.E. Olson, Dž. Belkić, C.L. Cocke, and H. Schmidt-Böcking. *Phys. Rev. Lett.*, 79:387–90, 1997.
13. John S. Briggs and Knud Taulbjerg. *J. Phys.*, B12:2565–73, 1979.
14. Robin Shakeshaft and Larry Spruch. *Rev. Mod. Phys.*, 51:369–405, 1979.
15. Dževad Belkić. *Nucl. Instr. Meth.*, B99:218–24, 1995.